www.amlett.com, www.vbripress.com/aml, DOI: 10.5185/amlett.2015.5629 Published online by the VBRI press in 2015

# Evaluation of antioxidant and antibacterial activity of various aspect ratio gold (Au) nanorods

**Shyamalima Sharma[1], Ajay Kumar Manhar[2], Pritom Jyoti Bora[3], Swapan Kumar Dolui[1*], Manabendra Mandal[2]**

[1]*Department of Chemical Sciences, Tezpur University, Napaam, Tezpur, Assam 784028, India*
[2]*Department of Molecular Biology and Biotechnology, Tezpur University, Napaam, Tezpur, Assam 784028, India*
[3]*Department of Physics, Tezpur University, Napaam, Tezpur, Assam 784028, India*

[*]Corresponding author. Tel: (+91) 9957198489; E-mail: swapandolui@gmail.com

**Received: 04 September 2014, Revised: 02 November 2014 and Accepted: 12 November 2014**

## ABSTRACT

In the current scenario, metal nanoparticles acquire much attention in terms of their diverse applications because of their extremely small size and large surface to volume ratio. Hence, our present study deals with the investigation of antioxidant and antibacterial activity of gold (Au) nanoparticles. First, anisotropic Au nanorods with various aspect ratios have been synthesized by a standard seeded growth method using CTAB-coated Au seed nanoparticles with size less than 10 nm as nucleation centre. Characterization of synthesized nanorods is made using UV-visible and TEM analysis. The antioxidant and antibacterial activities of Au nanorods have been investigated using 1,1-diphenyl-2-picrylhydrazyl (DPPH) as free radical source and Agar-well diffusion assay. The radical scavenging reaction of nanorods was monitored by a UV-visible spectrophotometer and found that Au nanorods show better antioxidant activity than spherical seeds due to the presence of more number of atoms as well as active sites for interaction with the free radical of DPPH. For a set of nanorods DPPH scavenging percentage is 80-90, while for seeds it is only 30. Again, very less amount (volume) of high aspect ratio nanorods is required for efficient scavenging. A linear relationship is observed between DPPH scavenging percentage and volume of Au nano-dispersions. The synthesized Au nanoparticles also have potent antibacterial activity, the maximum zone of inhibition (20 mm) is observed for longer nanorods, against indicator strains due to the interaction of more number of $Au^{+}$ cations to the negatively charged bacterial cell wall that causes rupturing of the cell wall and finally death. The minimum inhibitory concentration (MIC) for nanorods is lower when tested against gram negative bacteria viz. *Y. enterocolitica* (12.5μg/ml), *S. enterica typhimurium* (15 μg/ml), and *K. pneumoniae* (10 μg/ml) as compared to gram positive bacteria viz. S. aureus (20 μg/ml), *L. monocytogenes* AMDK2 (20 μg/ml) and *B. cereus* AMDK1 (25 μg/ml). From this study, it is concluded that high aspect ratio Au nanorods can act as an effective antioxidant and antibacterial agent and it makes the nanoparticles as an alternative for the development of new biomedical drugs in near future. Copyright © 2015 VBRI press.

**Keywords:** Antibacterial; antioxidant; nanocrystal; DPPH.

**Shyamalima Sharma**: Shyamalima Sharma is pursuing her doctorate degree with Prof. Swapan K. Dolui in the Department of Chemical Sciences, Tezpur University, Assam, India. Her research area of interest includes synthesis of anisotropic nanoparticles and their composites with different polymers and study of their application in various fields like biomedical, catalytic and in solar photovoltaics.

**Swapan K. Dolui**: Swapan K. Dolui is a professor in the Department of Chemical Sciences, Tezpur University, Assam, India. He pursued his PhD degree from IIT, Kharagpur, West Bengal, India. His area of research interest includes Liquid crystal polymer, sol-gel process, photopolymerization, emulsion polymerization, polymerization in supercritical carbon dioxide, olefin polymerization using Ziegler Natta Catalyst, conducting hydrogels, vegetable oil based alkyd resins, conducting polymers, nanocomposites, core shell polymers, conjugated polymer based solar cells, and electroluminescence of pi-conjugated polymer etc. Till date he has more than hundred twenty publications in peer reviewed journals.

 

## Introduction

Numerous essential free radical species are generated in our body during cellular metabolism; those are responsible for cellular signaling, pathogen defense and homeostasis etc. But excessive free radical generation causes damages to the living organisms. For instance, free radical oxygen species attack directly on unsaturated fatty acids in the cell membrane causing damages to the cells. So, in this regard an antioxidant plays a crucial rule. An antioxidant may terminate the oxidative potentiality by scavenging the free radical which is generated during oxidation process **[1]**. To date, large number of natural and synthetic antioxidants has been investigated to inhibit these oxidation reactions. Natural antioxidants such as Vitamins (A, C, E) and carotenoids can generate a stable intermediate by accepting an unpaired electron. These intermediates, being stable for a long time, interact in a controlled fashion, thus preventing auto oxidation and the energy of excess electron is dissipated without damage to the tissues. Such natural antioxidants can be recycled. On the contrary, due to the carcinogenicity of the synthetic antioxidants such as butylated hydroxyl toluene, tertiary butylated hydroquinone and gallic acid esters, they have limited uses **[2, 3]**.

Recently, some progresses have been achieved in the evaluation of antioxidant activity of nano materials **[4, 5]**. An attempt was made to explore the antioxidant and antibacterial activity of copper oxide (CuO) nanoparticles **[6]**. It was reported that CuO nanoparticles show free radical scavenging activity up to 85% in 1 h which is relatively higher in comparison to other metal oxide nanoparticles. Another work reported an efficient free radical scavenging property of starch assisted "green" silver nanoparticles **[7]**. Due to the physicochemical and optoelectronic properties of anisotropic Au nanoparticles, they find potent applications in catalysis **[8-10]**, biosensing **[11]** and optics **[12]**. Au and other noble metal nanoparticles exhibit promising catalytic activities for radical scavenging reactions **[13, 14]**. Catalytic activity of an anisotropic metal nanoparticle is dependent primarily on their shape, because such particles are composed of a particular crystallographic plane that determines the fraction of active surface sites present in that particle and that is why, shape variation may tune the catalytic activity **[9]**. Several research groups have investigated the catalytic activity of various metal and metal oxide nanoparticles. Recently the catalytic activity of $Au/TiO_2$ nanocomposites using various anisotropic $TiO_2$ nanoparticles was investigated for DPPH radical scavenging reaction and it was found that rod-like $TiO_2$ provided a higher activity than spherical one **[10]**. Again, it was established that the catalytic activity of polygonal Au nanoparticles is higher by a factor of 300–1000, in nitrophenol reduction compared to that of spherical Au nanoparticles **[9]**. Gold nanoparticles synthesized from the aqueous extract of red marine algae, Gracilaria corticata shows potent antioxidant and antimicrobial activity, which was reported in previous literature **[15]**. Although many literatures deal with catalytic activity of various anisotropic Au nanoparticles, a very few are found to investigate the effect of rod-like Au nanoparticles on radical scavenging reactions.

There are various bacteria that contaminate food, medical devices or any other environment which can grow to become a serious risk to human health. Some of the recognized guilty parties are *Bacillus cereus, Listeria monocytogenes, Yersinia enterocolitica*, *Staphylococcus spp*. and *Salmonella spp.* (contamination of food), *Staphylococcus aureus* and *Klebsiella pneumoniae* (prevalent in the hospital and medical environment). Although antibiotics have been used to great concern against pathogenic bacteria, most bacterial strains have now developed resistance to those through genetic mutations account for considerably potential threat **[16, 17]**. Although many methods for treating bacterial infections are currently available, there is an urgent requirement for new and improved approaches for bacterial destruction. Owing to the extremely small size and large surface to volume ratio, metal nanoparticles have been getting much attention in recent times towards various applications; remarkably in the field of nanobiotechnology **[18-20]** Nanoparticles have an enlarged contact area with micro-organisms that facilitates their biological and chemical activity. Another important feature of metal nanoparticles is their ability to target different bacterial structures that can make them an efficient antibacterial candidate for practical purposes **[21]**. Among various metal nanoparticles, Au nanoparticles are well-suited for a wide range of biological applications because of its chemical inertness and resistance to surface oxidation **[18, 22**]. The surfaces of Au nanoparticles are particularly suitable to serve as a stable and non-toxic platform, on which pharmaceutical compounds can be delivered **[22]**.

In this report, we focus narrowly on the potential of using Au nanoparticles for the control of pathogenic bacteria indicator strains as well as to scavenge radicals formed during cellular metabolism. To study the scavenging activity we have taken DPPH as the radical source and Agar-well diffusion assay for antibacterial measurements. At the end of this report, the effect of anisotropy as well as aspect ratio of nanoparticles on antioxidant and antibacterial activity has been thoroughly investigated, that can make the high aspect ratio Au nanorods as the most promising candidate for bio medical applications.

## Experimental

### *Materials*

Sodium borohydride ($NaBH_4$), cetyl trimethyl ammonium bromide (CTAB), ascorbic acid and methanol were purchased from Merck India. Silver nitrate ($AgNO_3$) was purchased from Rankem. Chloroauric acid ($HAuCl_4$) and 2,2-Diphenyl-1-picrylhydrazyl hydrate (DPPH) were purchased from Sigma Aldrich India. All the chemicals were analytical grade and used without further purification. The indicator bacterial strains *S. aureus* (MTCC 3160), *Y. enterocolitica* (MTCC 859), *S. enterica typhimurium* (MTCC 1252), and *K. pneumoniae* (MTCC 618) were *procured* from the Institute of Microbial Technology (*IMTECH), India. Two bacterial strains viz. L. monocytogenes* AMDK2 (KF894986) and *B. cereus* AMDK1 (KC683896) were isolated from fermented milk product (curd) and fermented mustard (Kharoli) respectively. HiAntibiotic Zone Scale for measurement of zone of inhibition was purchased from HiMedia, Mumbai.

*Seeded growth method of synthesis of Au nanorods*

Preparation of seed solution: Au nanorods were synthesized by the method described by M. A. El-Sayed and his coworkers **[23]**. In this method CTAB solution (5ml, 0.2 M) was mixed with 5 ml of 0.001292 M $HAuCl_4$. To the stirred solution, 0.60 ml of ice cold 0.01 M $NaBH_4$ was added, which resulted in the formation of a brownish yellow solution. Vigorous stirring of the seed solution was continued for ~2 minutes.

Growth of nanorods: CTAB (5 mL, 0.20 M) was added to 0.25, 0.15, 0.05 mL of 0.0040M $AgNO_3$ solution at room temperature. To this solution, 5 mL of 0.0010 M $HAuCl_4$ was added and after gentle mixing of the solution 70µL of 0.0788 M ascorbic acid was added. Ascorbic acid acts as a mild reducing agent which changes the growth solution from dark yellow to colorless. It is worth noting that the above three solutions are identical except for their silver ion content. The concentrations of silver ion in the growth solution were $9.8x10^{-5}$M, $5.9x10^{-5}$M and $2.03x10^{-5}$M for 0.25 mL, 0.15 mL and 0.05 mL of 0.0040M $AgNO_3$ solution respectively. The final step was the addition of 12 µL of the seed solution to the growth solution at room temperature. The color of the solution has gradually changed within 10-20 min. For longer nanorods the color change takes place more slowly. Nanorods were separated from spherical and other shapes by centrifugation and re-dispersion process. The temperature of the growth medium was kept constant at room temperature in all the experiments. The overall reaction scheme of the seeded growth method is shown in **Fig. 1**.

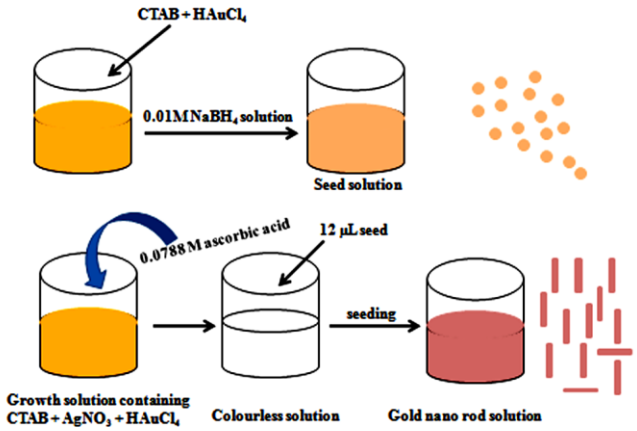


**Fig. 1.** Schematic representation, showing the seeded growth method of synthesis of Au nanorods.

*Measurements of antioxidant activity*

Antioxidant activity was measured by using the modified DPPH method as reported previously **[24]**. To examine the concentration effect of the Au seed solution and Au nanorods, 60µL, 120µL, 180µL, 240µL, 300µL, 360µL, 420µL, 480µL, 540µL and 600 µL of Au nano dispersion were mixed with 2mL of 100 µM DPPH nano-dispersion. The samples were vortexed and allowed to scavenge DPPH in dark for 5 min. The absorbance of the supernatants after centrifugation at 9200 rpm for 2 min was measured at 517nm in UV–visible spectrophotometer. The scavenging percentage was calculated using the formula:

$$\text{DPPH scavenging (\%)} = \frac{(Ac - As)x\ 100}{Ac} \quad (1)$$

where, Ac and As are the intensity of peak at 517 nm for control (DPPH) and supernatant DPPH solvent respectively.

*Antibacterial activity*

The antibacterial activity of the samples was tested using the Agar-well diffusion assay. Briefly, 100 µl of a log-phase culture of the test microbes ($10^6$–$10^7$ CFU/ml) were seeded on the surface of Muller Hinton agar. Using a sterile borer, 8 mm-diameter wells were punched into the surface. In each plate, 50 µl of sample solution was loaded in all the four wells and in the fifth well, 15 µl gentamicin sulphate (1mg/ml) loaded was used as a positive control. The culture plates were incubated at 37 °C for 24 h. Studies were performed in triplicates and the observed zones of inhibition were measured using a HiAntibiotic Zone Scale. To determine the minimum inhibitory concentration (MIC) leading to the inhibition of bacterial growth **[25]**, microtitration plates were used for the tests. The samples were diluted with 100 µl of Mueller–Hinton broth inoculated with the tested bacteria at a concentration of $10^5$ CFU/ml. The MIC was read after 24 h of incubation at 37 °C as the MIC of the tested substance that inhibited the growth of the bacterial strain. The dispersions were used in the form in which they had been prepared.

*Characterization tools*

The morphology as well as size of the Au nanoparticles is investigated by transmission electron microscope (JEM 2100) with an acceleration voltage of 200 kV. The UV–visible absorption spectra of the samples taking water and THF as solvents were recorded in the range 200–800 nm using Shimadzu UV-2550 UV–visible spectrophotometer.

## Results and discussion

*Size and morphology using TEM analysis*

Representative TEM images of Au seed dispersion and a set of nanorods prepared at two different silver ion concentrations ($2.03x10^{-5}$M and $9.8x10^{-5}$M) are shown in **Fig. 2** and **Fig. 3**. Spherical seed particles with diameter ~10 nm are formed during the preliminary step of the reaction, shown in **Fig. 2**. TEM images of the nanorods (**Fig. 3**) show the average diameter of particles is 15-17 nm. **Fig. 3a** shows that in the nanoparticles prepared at $2.03x10^{-5}$M silver ion concentration, growth of nanorods is incomplete with an aspect ratio of 1.4-2.4. TEM micrograph of the Au nanorods prepared at $9.8x10^{-5}$M silver ion concentration (**Fig. 3b**) shows a well-defined nanoscaling and highly mono dispersed, capsule shaped Au nanorods formation is observed with a low polydispersity index. It is apparent that the size of the nanorods is less than 20 nm with an aspect ratio in the range 2.5-3.5.

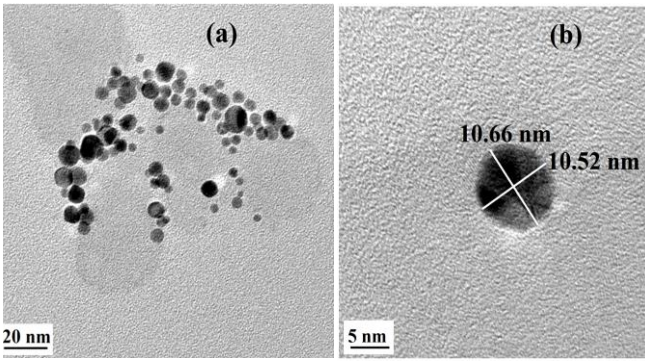


**Fig. 2.** TEM images of (a) Au seed solution and (b) a single spherical nanoparticle showing the diameter.

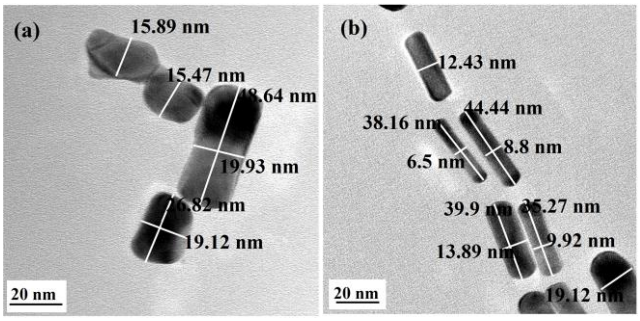


**Fig. 3.** TEM images of (a) Au nanorod (at $2.03x10^{-5}$M $Ag^{+}$) and (b) Au nanorod (at $9.8x10^{-5}$M $Ag^{+}$).

*Optical characterization: Ultraviolet-visible (UV-visible) analysis*

The UV-visible spectra of Au seeds and Au nanorods at $13.3x10^{-5}$M, $9.8x10^{-5}$M, $5.9x10^{-5}$M and $2.03x10^{-5}$M silver ion concentration are shown in **Fig. 4**. Au seed solution gives an absorption maximum at ~522 nm which is due to the surface plasmon resonance of the spherical Au nanoparticles **[26, 27]**. In contrast to the spherically symmetric Au nanoparticles, in the Au nanorods electron oscillation occurs across and along the long axis of the nanorods, because of which they possess two different resonance modes at ~529 nm and ~650 nm under the UV-visible light exposure. These two modes are termed the transverse and longitudinal modes respectively **[27-29]**. Aspect ratio of the nanorods has a great influence on their longitudinal plasmon band. As we increase the silver ion concentration from $2.03x10^{-5}$M to $9.8x10^{-5}$M in the growth solution the transverse plasmon band shifts from ~529 nm to ~545 nm. This indicates that the aspect ratio of the nanorods increases with increase in silver ion concentration. But at a certain higher concentration of silver ion ($13.3x10^{-5}$M) the plasmon band shows a reverse trend (absorption maximum at ~540nm). This may be due to the interaction of silver ion with the bromide ion of the structure directing agent (CTAB) **[23]**. The silver ions are adsorbed at the Au nanoparticle surface in the form of silver bromide (AgBr) that restricts the growth and stabilize the surface. Same trend is also observed in the case of longitudinal plasmon band. Therefore, in the synthesis procedure the optimum concentration of silver ion is $9.8x10^{-5}$M.

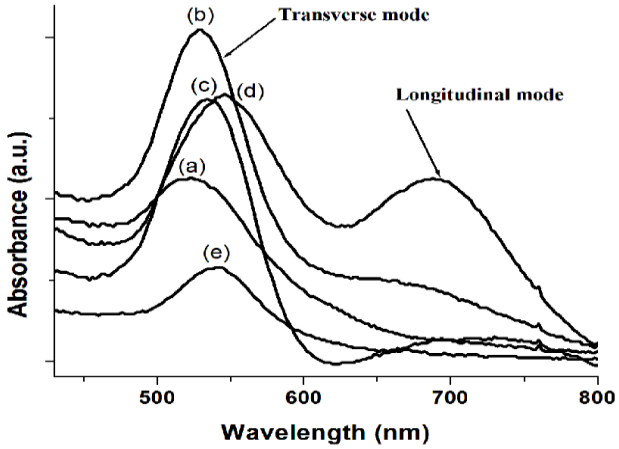


**Fig. 4.** UV-Visible spectra of (a) Au-seed solution and Au nanorods containing (b) $2.03x10^{-5}$M, (c) $5.9x10^{-5}$M, (d) $9.8x10^{-5}$M, (e) $13.3x10^{-5}$M $Ag^{+}$.

*Antioxidant activity*

DPPH is widely used for testing preliminary radical scavenging activity of a compound or a nanoparticle. In the present study the synthesized Au nanorods show potential free radical scavenging activity and the use of DPPH provides an easy and rapid way to evaluate antioxidant activity. The DPPH scavenging reactions are shown in **Fig. 5** and **Fig. 6** for different Au nano-dispersion.

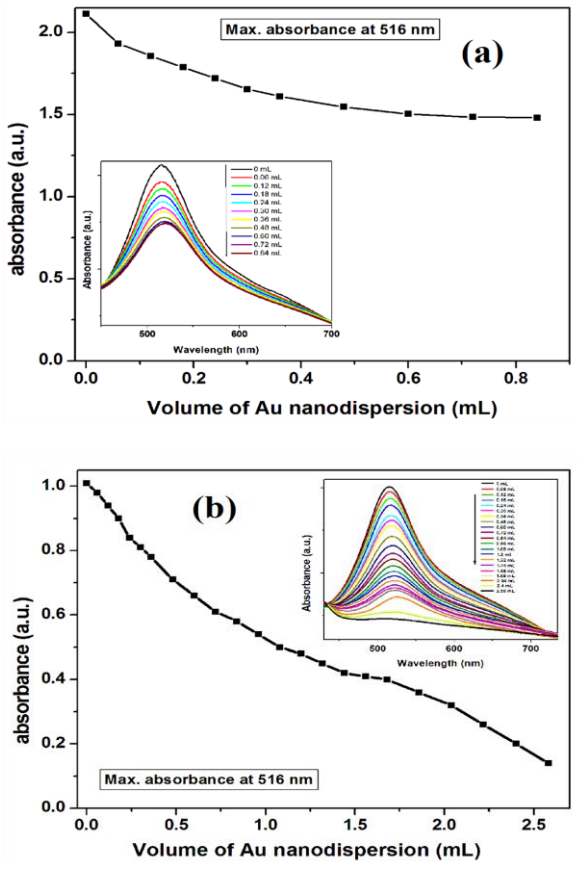


**Fig. 5.** Free radical scavenging reaction of (a) Au seed dispersion, (b) Au nanorods containing $2.03x10^{-5}$M $Ag^{+}$.

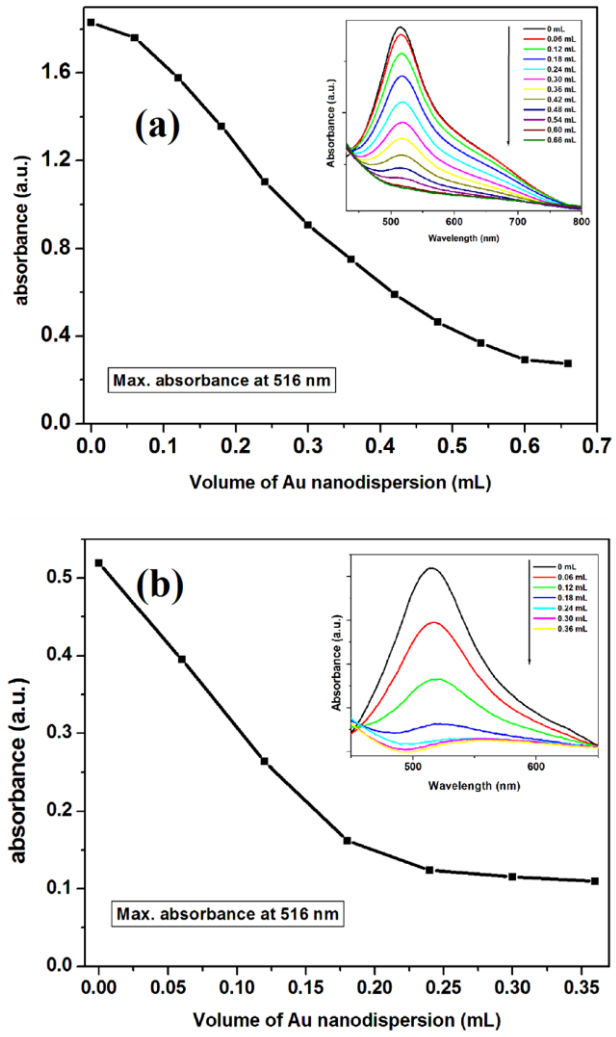


**Fig. 6.** Free radical scavenging reaction of Au nanorods containing (a) 5.9x10$^{-5}$M $Ag^{+}$, (b) 9.8x10$^{-5}$ M $Ag^{+}$.

From the graph of DPPH scavenging in presence of Au seed solution (**Fig. 5a**), the DPPH scavenging percentage is found to be only 30, whereas in case of nanorod dispersions the scavenging percentage is found to be 80-90 (**Fig. 5b** and **Fig. 6 a-b**). A morphological effect may contribute to the high catalytic activity of rod shaped Au nanoparticles. When the shape of particles deviates from spherical, the particular shape is composed of a particular crystallographic plane that determines the fraction of active surface sites present in that particle. Moreover, the electronic state of the metal varies with shape that causes variation in catalytic activity **[9]**. Another context may arise in terms of surface atoms. The fraction of surface atoms in Au nanorods is very large than in spherical seeds. Nanorods have large number of surface atoms at corners and edges and these surface atoms are responsible for high catalytic activity of these nanorods **[9]**. The free radical in DPPH probably attacks the nanoparticle surface at the corners and edges and as the nanorods have greater number of surface atoms at corners and edges the scavenging activity is more in case of these nanoparticles.

**Fig. 5b** and **Fig. 6a-b** show DPPH scavenging of Au nanorods with different aspect ratios. With increasing the aspect ratio the fraction of surface atoms at corners and edges increases. As a consequence of this, with the inclusion of smaller concentration of nano dispersion, catalytic activity increases apparently which is clear from **Fig. 5** and **Fig. 6**. Comparing these spectra we have found that when we use shorter nano rod dispersion, a higher amount (2.58 mL) is required for 90% DPPH scavenging (**Fig. 5b**), whereas in case of longer nanorods a very less amount (0.36 mL) is needed for 80% DPPH scavenging (**Fig. 6b**). Longer nanorods have highest number of surface atoms at corners and edges. Therefore, a very less amount of the nano-dispersion can cause an effective scavenging of DPPH free radical.

**Fig. 7 (a)** shows the percentage scavenging of DPPH in presence of different Au nano-dispersion. The spectra show a linear relationship between volume of Au nano dispersion and their percentage scavenging. The bar diagram (**Fig. 7(b)**) indicates that the high aspect ratio Au nanorods have better scavenging activity than the spherical seeds and with increasing the length of nanorods the activity increases as well.

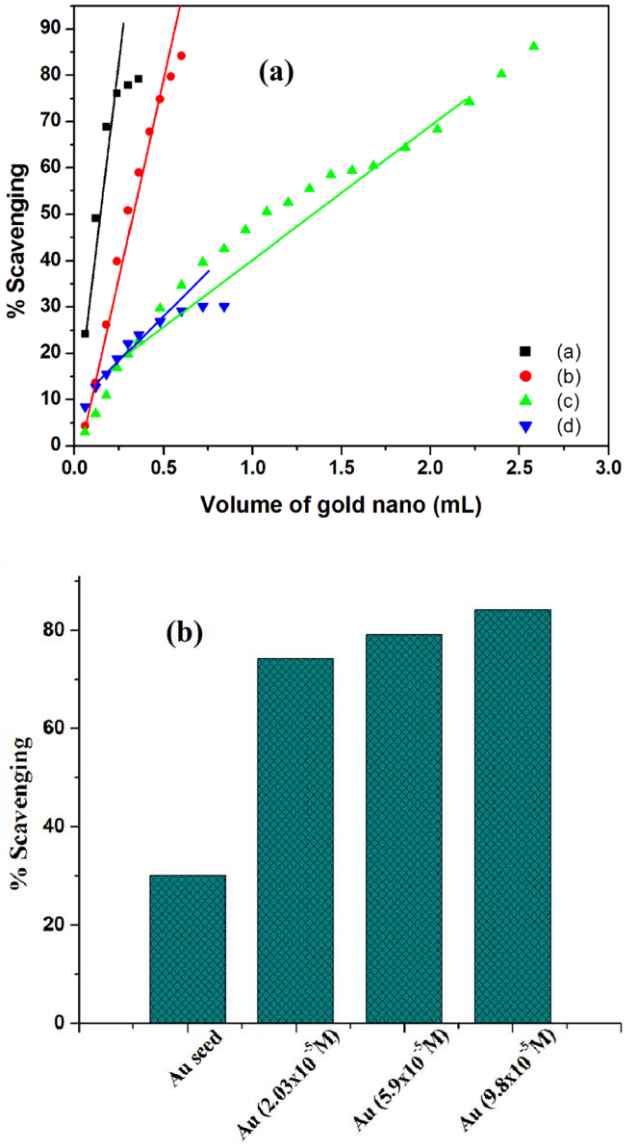


**Fig. 7.** (a) Graph showing volume vs % scavenging of Au nanorods dispersion containing (a) 5.9x10$^{-5}$M, (b) 9.8x10$^{-5}$M and (c) 2.03x10$^{-5}$M $Ag^{+}$ and (d) Au seed solution, (b) bar diagram showing a comparable relation among all the nanoparticle dispersion in terms of their percentage scavenging.

*Antibacterial activity*

The figures of all the samples in **Fig. 8** show significant antibacterial activity. However Au nanorods show slightly higher activity than spherical nanoparticles in terms of zone of inhibition due to more interaction with surface of bacterial cells because of more number of $Au^{+}$ cations are formed from Au nanorods. These cations can bind to the negatively charged bacterial cell wall thus rupturing the wall resulting in denaturation of protein and finally death **[30]**. Moreover, earlier reports have been suggested that due to the binding of Au nanoparticles or $Au^{+}$ ions, outer membrane of the cell wall is destabilized as well as the plasma membrane is ruptured thereby causing the depletion of intracellular ATP **[31, 34]**. Since, the antibacterial activity is directly proportional to the increase in the size of Au nanoparticles **[30]**, the maximum zone of inhibition (20 mm) was observed in longer nanorods, viz., nanorods at 5.9x10-5M $Ag^{+}$ and 9.8x10-5M $Ag^{+}$ against indicator strains tested (**Table 1**). The minimum inhibitory concentration (MIC) of Au nanoparticles is lower when tested against gram negative bacteria, viz. Y. enterocolitica (12.5 µg/ml), S. enteric typhimurium (15 µg/ml), and K. pneumoniae (10 µg/ml) bacteria as compared to gram positive bacteria, viz. S. aureus (20 µg/ml), L. monocytogenes AMDK2 (20 µg/ml) and B. cereus AMDK1(25 µg/ml). These results can be explained on the basis of the differences on the cellular wall of each strain. The cellular wall of gram-positive strains is composed of thicker peptidoglycan layer that consists of linear polysaccharide chains cross-linked by short peptides thus forming more rigid structure. Therefore, it is very difficult to penetrate the wall by the nanoparticle and therefore, MIC increases **[19]**. Gram negative bacteria possess thinner peptidoglycan layer, thus causing the easy penetration of Au nanoparticles into the cell wall. Reactive oxygen species (ROS)-independent mechanism of action of Au nanoparticles suggests their low toxicity to mammalian cells **[33]**.

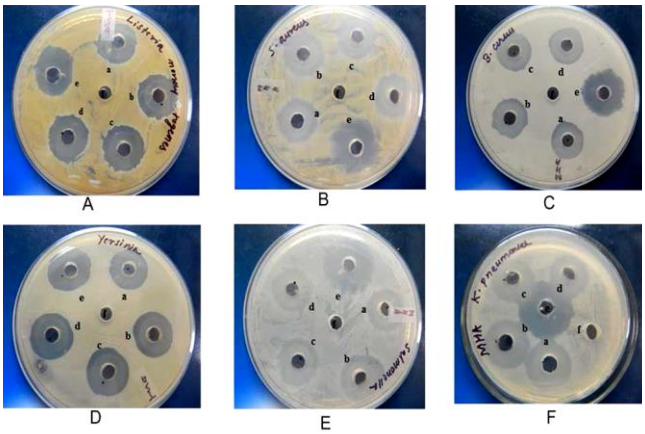


**Fig. 8.** Antibacterial activity of Au nanorods against Gram-positive bacteria viz. (A) L. monocytogenes AMDK2 (KF894986), (B) S. aureus (MTCC 3160), (C) B. cereus AMDK1 (KC683896), and against Gram-negative bacteria viz. (D) Y. enterocolitica (MTCC 859), (E) S. enterica typhimurium (MTCC 1252), (F) K. pneumoniae (MTCC 618). The plate shows zone of inhibition by samples represented by a) Au seed (spherical), b) Au nanorods (2.05x10-5M), c) Au nanorods (5.9x10-5M), d) Au nanorods (9.8x10-5M), e) Gentamicin sulphate (1mg/ml) as a positive control and f) water as a negative control.

**Table 1.** Diameter of inhibition zone against various microbial strains. The measurement expressed in mm is the mean of three replicates, Gentamicin sulphate (1mg/ml) served as a positive control.

| Strains | Positive Control (mm) | Au seed spherical (mm) | Au nanorods ($2.05x10^{-5}$M) | Au nanorods ($5.9x10^{-5}$M) | Au nanorods ($9.8x10^{-5}$M) |
|---|---|---|---|---|---|
| Y. Enterocolitica (MTCC 859) | 20 | 18 | 19 | 20 | 20 |
| S. Enterica typhimurium (MTCC 1252) | 21 | 17 | 17 | 18 | 18 |
| K. pneumoniae (MTCC 618) | 23 | 18 | 19 | 19 | 20 |
| *B. cereus* AMDK1 (KC683896) | 20 | 16 | 17 | 18 | 18 |
| L. monocytogenes AMDK2 (KF894986) | 18 | 18 | 19 | 20 | 20 |
| S. aureus (MTCC 3160) | 20 | 18 | 19 | 20 | 20 |

## Conclusion

Au nanorods of various aspect ratios have been successfully synthesized by a seeded growth method using pre-synthesized Au nanoparticles (~10nm diameter) as a seed for nanocrystal growth. Well-defined and highly mono-dispersed capsule shaped nanorods, with diameter less than 20 nm and 1.4-3.5 aspect ratio have been observed in TEM analysis. Au nanorods show better antioxidant activity than spherical seeds due to the presence of more number of atoms as well as active sites that are responsible for the interaction with the free radical of DPPH. While for Au seeds DPPH scavenging percentage is only 30, for a set of Au nanorods it is 80-90. Again, very less amount of high aspect ratio nanorods can cause more efficient scavenging than the shorter nanorods. The DPPH scavenging percentage linearly increases with increase in volume of Au nano-dispersions. Again, from the antibacterial measurement we can conclude that all the samples show significant antibacterial activity. However, the activity is higher in case of Au nanorods than spherical nanoparticles in terms of zone of inhibition, which is due to the interaction of more number of $Au^{+}$ cations to the negatively charged bacterial cell wall that causes rupturing of the cell wall and finally death. Similar explanation can be made for high aspect ratio nanorods that shows bigger zone of inhibition. Moreover, the MIC of Au nanoparticles is lower when tested against gram negative bacteria (~10-15 µg/ml) as compared to gram positive bacteria (~20-25µg/ml) because of thinner peptidoglycan layer present in gram negative bacteria that offers easy penetration of Au nanoparticles into the wall. Thus, summarizing all the findings, it can be concluded that high aspect ratio Au nanorods can act as an effective antioxidant and antibacterial agent thus making the nanoparticle as an alternative for the development of new biomedical drugs in near future.

**Acknowledgements**

This work was financially supported by the Department of Electronics and Information Technology, New Delhi, India (Sanction No. 1(11)/2012-EMCD dated 5.3.2013). Authors also acknowledge SAIF, North-Eastern Hill University, India and SAIC, Tezpur University, India for analytical support.

  

**Reference**


1. Beltran, E.; Pla, R.; Yuste, J.; Mor-Mur, M.; *Meat Science* **2004**, *66*, 719. **DOI:** 10.1016/j.meatsci.2003.07.004
2. Anagnostopoulou, M. A.; Kefalas, P.; Papageorgiou, V. P.; Assimopoulou, A. N.; Boskou, D.; *Food Chem.* **2006**, *94*, 19. **DOI:** 10.1016/j.foodchem.2004.09.047
3. Medhe, S.; Bansal, P.; Srivastava, M. M.; *Appl. Nanosci.* **2014**, *4*, 153. **DOI:** 10.1007/s13204-012-0182-9
4. Abdel-Aziz, M. S.; Shaheen, M. S.; El-Nekeety, A. A.; Abdel-Wahhab, M. A.; *J Saudi Chem. Soc.* **2014**, *18*, 356. **DOI:** 10.1016/j.jscs.2013.09.011
5. Martın, R.; Menchon, C.; Apostolova, N.; Victor, V. M.; Alvaro, M.; Herance, J. R.; Garcia, H.; *ACS Nano* **2010**, *4*, 6957. **DOI:** 10.1021/nn1019412.
6. Das, D.; Nath, B. C.; Phukon, P.; Dolui, S. K.; *Colloids Surf. B* **2013**, *101*, 430. **DOI:** 10.1016/j.colsurfb.2012.07.002
7. Konwarh, R.; Gogoi, B.; Philip, R.; Laskar, M.A.; Karak, N.; *Colloids Surf. B* **2011**, *84*, 338. **DOI:** 10.1016/j.colsurfb.2011.01.024
8. Chirea, M.; Freitas, A.; Vasile, B. S.; Ghitulica, C.; Pereira, C. M.; Silva, F.; *Langmuir* **2011**, *27*, 3906. **DOI:** 10.1021/la104092b
9. Rashid, M. H.; Mandal, T. K.; *Adv. Funct. Mater.* **2008**, *18*, 2261. **DOI:** 10.1002/adfm.200800085
10. Isono, R.; Yoshimura, T.; Esumi, K.; *J. Colloid Interface Sci.* **2005**, *288*, 177. **DOI:** 10.1016/j.jcis.2005.02.078
11. Wang, X.; Zou, M.; Huang, H.; Ren, Y.; Li, L.; Yang, X.; Li, N.; *Biosens. Bioelectron.* **2013**, *41*, 569. **DOI:** 10.1016/j.bios.2012.09.023
12. Nehl, C. L.; Liao, H.; Hafner, J. H.; *Nano Lett.* **2006**, *6*, 683. **DOI:** 10.1021/nl052409y
13. Esumi, K.; Takei, N.; Yoshimura, T.; *Colloids Surf. B* **2003**, *32*, 117. **DOI:** 10.1016/S0927-7765(03)00151-6
14. Esumi, K.; Houdatsu, H.; Yoshimura, T.; *Langmuir* **2004**, *20*, 2536. **DOI:** 10.1021/la036299r
15. Naveena, B. E.; Prakash, S.; *Asian J. Pharm. Clin. Res.* **2013**, *6*, 179. **ISSN:** 0974-2441.
16. Leeb, M.; *Nature* **2004**, *431*, 892. **DOI:** 10.1038/431892a
17. Norrby, S. R.; Nord, C. E.; Finch, R.; *Lancet Infect. Dis.* **2005**, *5*, 115. **DOI:** 10.1016/S1473-3099(05)01283-1
18. Prema, P.; Thangapandiyan, S.; *Int. J. Pharm. Pharm. Sci.* **2013**, *5*, 310. **ISSN:** 0975-1491.
19. Priyadarshini, S.; Gopinath, V.; Priyadharsshini, N. M.; MubarakAli, D.; Velusamy, P.; *Colloids Surf. B* **2013**, *102*, 232. **DOI:** 10.1016/j.colsurfb.2012.08.018
20. Puiso, J.; Jonkuviene, D.; Macioniene, I.; Salomskiene, J.; Jasutiene, I.; Kondrotas, R.; *Colloids Surf. B* **2014**, *121*, 214. **DOI:** 10.1016/j.colsurfb.2014.05.001
21. Gordon, O.; Slenters, T. V.; Brunetto, P. S.; Villaruz, A. E.; Sturdevant, D. E.; Otto, M.; Landmann, R.; Fromm, K. M.; *Antimicrob. Agents Chemother.* **2010**, *54*, 4208. **DOI:** 10.1128/AAC.01830-09
22. Pissuwan, D.; Cortie, C. H.; Valenzuela, S. M.; Cortie, M. B.; *Trends Biotechnol.* **2010**, *28*, 207. **DOI:** 10.1016/j.tibtech
23. Nikoobakht, B.; El-Sayed, M. A.; *Chem. Mater.* **2003**, *15*, 1957. **DOI:** 10.1021/cm0207321
24. Serpen, A.; Capuano, E.; Fogliano, V.; Gokmen, V.; *J. Agric. Food Chem.* **2007**, *55*, 7676. **DOI:** 10.1021/jf071291z
25. Wiegand, I.; Hilpert, K.; Hancock, R. E. W.; *Nature Protocols* **2008**, *3*, 163. **DOI:** 10.1038/nprot.2007.521
26. Delapierre, M. T.; Majimel, J.; Mornet, S.; Duguet, E.; Ravaine, S. *Gold. Bull.* **2008**, *41*, 195. **ISSN:** 1027-8591
27. Daniel, M. C.; Astruc, D.; *Chem. Rev.* **2004**, *104*, 293. **DOI:** 10.1021/cr030698
28. Jana, N. R.; Gearheart, L.; Murphy, C. J.; *J. Phys. Chem. B* **2001**, *105*, 4065. **DOI:** 10.1021/jp0107964
29. Jana, N. R.; Gearheart, L.; Murphy, C. J.; *Chem. Mater.* **2001**, *13*, 2313. **DOI:** 10.1021/cm000662n
30. Lin, Y. S. E.; Vidic, R. D.; Stout, J. E.; McCartney, C. A.; Yu, V. L.; Water Res. **1998**, *32*, 1997. **DOI:** 10.1016/S0043-1354(97)00460-0
31. Lok, C. N.; Ho, C. M.; Chen, R.; He, Q. Y.; Yu, W. Y.; Sun, H.; Tam, P. K. H.; Chiu, J. F.; Che, C. M.; *J. Proteome Res.* **2006**, *5*, 916. **DOI:** 10.1021/pr0504079
32. Badwaik, V. D.; Vangala, L. M.; Pender, D. S.; Willis, C. B.; Aguilar, Z. P.; Gonzalez, M. S. Paripelly, R.; Dakshinamurthy, R.; *Nanoscale Res. Lett.* **2012**, *7*, 1. **DOI:** 10.1186/1556-276X-7-623
33. Zhao, Y.; Tian, Y.; Cui, Y.; Liu, W.; Ma, W.; Jiang, X.; *J. Am. Chem. Soc.* **2010**, *132*, 12349. **DOI:** 10.1021/ja1028843
34. Rai, A.; Prabhune, A.; Perry, C. C.; *J. Mater. Chem.* **2010**, *20*, 6789. **DOI:** 10.1039/c0jm00817f